Search for the decay $B^0 \rightarrow \gamma\gamma$

S. Villa,[13] K. Abe,[5] K. Abe,[38] I. Adachi,[5] H. Aihara,[40] Y. Asano,[43] T. Aushev,[9] S. Bahinipati,[3] A. M. Bakich,[35]
V. Balagura,[9] E. Barberio,[16] A. Bay,[13] I. Bedny,[1] K. Belous,[8] U. Bitenc,[10] I. Bizjak,[10] A. Bondar,[1] A. Bozek,[22]
M. Bračko,[5,15,10] T. E. Browder,[4] Y. Chao,[21] A. Chen,[19] W. T. Chen,[19] B. G. Cheon,[2] R. Chistov,[9] Y. Choi,[34] A. Chuvikov,[29]
S. Cole,[35] J. Dalseno,[16] M. Danilov,[9] M. Dash,[44] A. Drutskoy,[3] S. Eidelman,[1] N. Gabyshev,[1] A. Garmash,[29] T. Gershon,[5]
G. Gokhroo,[36] B. Golob,[14,10] J. Haba,[5] T. Hara,[26] K. Hayasaka,[17] M. Hazumi,[5] L. Hinz,[13] T. Hokuue,[17] Y. Hoshi,[38]
S. Hou,[19] W.-S. Hou,[21] K. Ikado,[17] A. Imoto,[18] K. Inami,[17] R. Itoh,[5] M. Iwasaki,[40] Y. Iwasaki,[5] C. Jacoby,[13] J. H. Kang,[45]
P. Kapusta,[22] T. Kawasaki,[23] H. R. Khan,[41] H. Kichimi,[5] S. K. Kim,[32] S. M. Kim,[34] K. Kinoshita,[3] S. Korpar,[15,10]
P. Krokovny,[1] R. Kulasiri,[3] C. C. Kuo,[19] A. Kuzmin,[1] Y.-J. Kwon,[45] G. Leder,[7] T. Lesiak,[22] S.-W. Lin,[21] D. Liventsev,[9]
T. Matsumoto,[42] W. Mitaroff,[7] H. Miyata,[23] Y. Miyazaki,[17] R. Mizuk,[9] D. Mohapatra,[44] I. Nakamura,[5] E. Nakano,[25]
M. Nakao,[5] Z. Natkaniec,[22] S. Nishida,[5] S. Ogawa,[37] T. Ohshima,[17] T. Okabe,[17] S. Okuno,[11] S. L. Olsen,[4] H. Ozaki,[5]
H. Palka,[22] C. W. Park,[34] K. S. Park,[34] R. Pestotnik,[10] L. E. Piilonen,[44] Y. Sakai,[5] N. Sato,[17] N. Satoyama,[33]
T. Schietinger,[13] O. Schneider,[13] C. Schwanda,[7] R. Seidl,[30] K. Senyo,[17] M. E. Sevior,[16] M. Shapkin,[8] H. Shibuya,[37]
A. Somov,[3] N. Soni,[27] R. Stamen,[5] S. Stanič,[24] M. Starič,[10] T. Sumiyoshi,[42] K. Tamai,[5] N. Tamura,[23] M. Tanaka,[5]
G. N. Taylor,[16] Y. Teramoto,[25] X. C. Tian,[28] K. Trabelsi,[4] T. Tsukamoto,[5] S. Uehara,[5] T. Uglov,[9] K. Ueno,[21] S. Uno,[5]
P. Urquijo,[16] G. Varner,[4] K. E. Varvell,[35] C. C. Wang,[21] C. H. Wang,[20] Y. Watanabe,[41] J. Wicht,[13] E. Won,[12] Q. L. Xie,[6]
B. D. Yabsley,[35] A. Yamaguchi,[39] M. Yamauchi,[5] J. Ying,[28] L. M. Zhang,[31] Z. P. Zhang,[31] and D. Zürcher[13]

(The Belle Collaboration)

[1]*Budker Institute of Nuclear Physics, Novosibirsk*
[2]*Chonnam National University, Kwangju*
[3]*University of Cincinnati, Cincinnati, Ohio 45221*
[4]*University of Hawaii, Honolulu, Hawaii 96822*
[5]*High Energy Accelerator Research Organization (KEK), Tsukuba*
[6]*Institute of High Energy Physics, Chinese Academy of Sciences, Beijing*
[7]*Institute of High Energy Physics, Vienna*
[8]*Institute of High Energy Physics, Protvino*
[9]*Institute for Theoretical and Experimental Physics, Moscow*
[10]*J. Stefan Institute, Ljubljana*
[11]*Kanagawa University, Yokohama*
[12]*Korea University, Seoul*
[13]*Swiss Federal Institute of Technology of Lausanne, EPFL, Lausanne*
[14]*University of Ljubljana, Ljubljana*
[15]*University of Maribor, Maribor*
[16]*University of Melbourne, Victoria*
[17]*Nagoya University, Nagoya*
[18]*Nara Women's University, Nara*
[19]*National Central University, Chung-li*
[20]*National United University, Miao Li*
[21]*Department of Physics, National Taiwan University, Taipei*
[22]*H. Niewodniczanski Institute of Nuclear Physics, Krakow*
[23]*Niigata University, Niigata*
[24]*Nova Gorica Polytechnic, Nova Gorica*
[25]*Osaka City University, Osaka*
[26]*Osaka University, Osaka*
[27]*Panjab University, Chandigarh*
[28]*Peking University, Beijing*
[29]*Princeton University, Princeton, New Jersey 08544*
[30]*RIKEN BNL Research Center, Upton, New York 11973*
[31]*University of Science and Technology of China, Hefei*
[32]*Seoul National University, Seoul*
[33]*Shinshu University, Nagano*
[34]*Sungkyunkwan University, Suwon*
[35]*University of Sydney, Sydney NSW*
[36]*Tata Institute of Fundamental Research, Bombay*

[37]*Toho University, Funabashi*
[38]*Tohoku Gakuin University, Tagajo*
[39]*Tohoku University, Sendai*
[40]*Department of Physics, University of Tokyo, Tokyo*
[41]*Tokyo Institute of Technology, Tokyo*
[42]*Tokyo Metropolitan University, Tokyo*
[43]*University of Tsukuba, Tsukuba*
[44]*Virginia Polytechnic Institute and State University, Blacksburg, Virginia 24061*
[45]*Yonsei University, Seoul*

The rare decay $B^0 \rightarrow \gamma\gamma$ is searched for in 104 fb^{-1} of data, corresponding to $111 \times 10^6 B\bar{B}$ pairs, collected with the Belle detector at the KEKB asymmetric-energy e^+e^- collider. No evidence for the signal is found, and an upper limit of 6.2×10^{-7} at 90% confidence level is set for the corresponding branching fraction.

The channel $B^0 \rightarrow \gamma\gamma$ is a rare decay of the B^0 meson that is interesting both experimentally, for its remarkably clean signature, and theoretically, as a tool for constraining physics beyond the standard model (SM). The SM prediction for the $B^0 \rightarrow \gamma\gamma$ branching fraction (BF) is around 3×10^{-8} [1], and a possible Feynman diagram contributing to this channel is shown in Fig. 1. Sizable enhancements of the BF are predicted in many new physics models [2]; a typical contribution arising from non-SM effects would follow from the replacement of the W boson in Fig. 1 with another charged particle such as a charged Higgs boson. The $B^0 \rightarrow \gamma\gamma$ channel is also interesting because it allows the study of nontrivial QCD dynamics in B decay, via a pure nonhadronic final state.

Experimental limits on the BF have been set by L3 [3] and *BABAR* [4]. The *BABAR* upper limit of 1.7×10^{-6} at 90% confidence level (CL), obtained with 19.4 fb^{-1} of data, is the most restrictive existing experimental constraint on this channel.

The present search for the $B^0 \rightarrow \gamma\gamma$ decay is based on a data sample of 104 fb^{-1}, which contains $111 \times 10^6 B\bar{B}$ pairs, collected with the Belle detector at the KEKB asymmetric-energy e^+e^- (3.5 on 8 GeV) collider [5] operating at the $\Upsilon(4S)$ resonance.

The Belle detector is a large-solid-angle magnetic spectrometer that consists of a 4-layer silicon vertex detector, a small-cell inner drift chamber [6], a 47-layer central drift chamber, an array of aerogel threshold Čerenkov counters, a barrel-like arrangement of time-of-flight scintillation
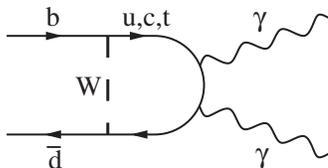

FIG. 1. A possible diagram contributing to $B^0 \rightarrow \gamma\gamma$ at the lowest order in the SM. The exchange of a charged Higgs boson instead of the W boson could contribute to this process in some extensions of the SM.

counters, and an electromagnetic calorimeter comprised of CsI(Tl) crystals located inside a superconducting solenoid coil that provides a 1.5 T magnetic field. An iron flux-return located outside of the coil is instrumented to detect K_L^0 mesons and to identify muons. The detector is described in detail elsewhere [7].

The $B^0 \rightarrow \gamma\gamma$ events are characterized in the center-of-mass (CM) frame by two back-to-back highly energetic photons. Photons are selected from isolated clusters in the calorimeter that are not matched to charged tracks. We require a shower shape consistent with that of a photon: for each cluster, the ratio of the energy deposited in the array of the central 3×3 calorimeter cells to that of 5×5 cells is computed, and clusters with a ratio smaller than 0.95 are rejected.

In the Belle detector, a large background for this channel is due to the overlap of a hadronic event with energy deposits left in the calorimeter by previous QED interactions (mainly Bhabha scattering). Such composite events are completely removed using timing information for calorimeter clusters associated with the candidate photons. Only photons that are in time with the rest of the event are retained. The efficiency of this selection on signal events is larger than 99.5%. The cluster timing information is stored in the raw data, and is available in the reduced format used for analyses only for data processed after the summer of 2004, thus limiting the data set available for this analysis to 104 fb^{-1}.

Rejection of π^0 and η mesons is of primary importance in a search for a purely radiative rare decay of the B^0 meson. All pairs of photons with energy larger than 50 MeV and a maximum absolute value of the difference between their invariant mass and the π^0 mass [8] of 15 MeV/c^2 are identified as neutral pions. For η mesons, the minimum energy requirement is 100 MeV, and the invariant mass of the two photons is required to be within 60 MeV/c^2 of the η mass [8]. All pairs of photons passing either the π^0 or η selection are removed from subsequent analysis.

The two highest-energy photons are selected and their momenta are added to reconstruct the B^0 momentum. Two variables are used to separate signal events from background: $M_{\mathrm{bc}} = \sqrt{E_{\mathrm{beam}}^{*2}/c^4 - p_B^{*2}/c^2}$ and $\Delta E = E_B^* - E_{\mathrm{beam}}^*$, where E_{beam}^* is the beam energy and E_B^* and p_B^* are the reconstructed B^0 energy and momentum, all variables being evaluated in the CM frame. The signal is concentrated near $\Delta E = 0$ and M_{bc} equal to the B^0 mass. The signal window is therefore defined as

$$-0.25 \text{ GeV} < \Delta E < 0.15 \text{ GeV}$$

$$5.272 \text{ GeV}/c^2 < M_{\mathrm{bc}} < 5.288 \text{ GeV}/c^2$$

corresponding to about 2 standard deviation intervals above and below the central values just mentioned.

The main background for the $B^0 \to \gamma\gamma$ channel is due to continuum events, mostly coming from light quark pair production and fragmentation ($u\bar{u}$, $d\bar{d}$, and $s\bar{s}$, uds for short). Two variables that display quite powerful separation between signal and continuum background are a Fisher discriminant based on modified Fox-Wolfram moments [9] and the B^0 production angle with respect to the beam in the CM frame, $\cos\theta_B^*$. These variables are combined in a likelihood ratio, LR; signal and background distributions used to construct the LR are extracted from Monte Carlo (MC) samples. In the continuum background, the two particles that are reconstructed as photons are more abundantly produced at low polar angle (θ^*, measured in the CM frame), while the signal photons have a flat distribution in $\cos\theta^*$. Selection requirements on LR (LR > 0.92) and on the cosine of the polar angle of the most energetic photon in the event ($|\cos\theta^*| < 0.65$) are optimized by maximizing $N_{\mathrm{sig}}/\sqrt{N_{\mathrm{sig}} + N_{\mathrm{bck}}}$, where N_{sig} (N_{bck}) is the expected number of signal (background) events in the
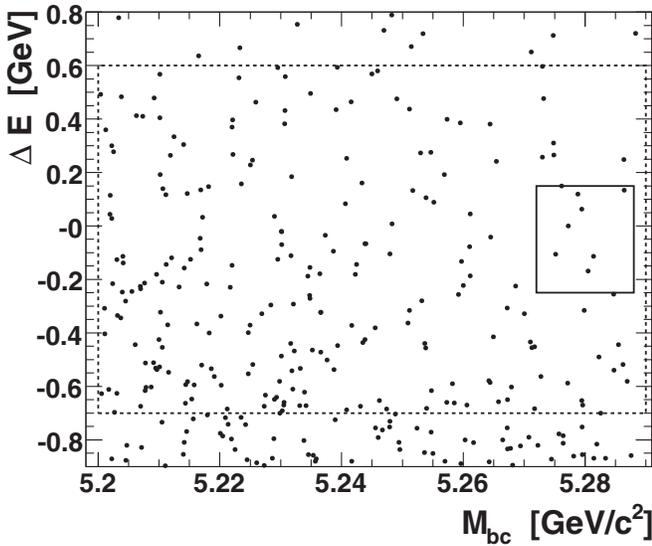

FIG. 2. ΔE versus M_{bc} for data events, selected as described in the text. Seven events are in the signal window (solid rectangle). The fit window is shown as a dashed rectangle.

signal window. The expected numbers of events are computed for an integrated luminosity of 104 fb^{-1} and assuming for the signal the BF predicted by the SM and for the background the prediction of the continuum MC. The above requirements reduce the continuum background in the signal window by a factor of 55, while retaining 31% of signal events.

The total selection efficiency for signal, evaluated using MC events, is 11.7%. In data, seven events lie in the signal window. They are shown in the ΔE–M_{bc} plane in Fig. 2, where the signal window is represented as a solid-border rectangle.

Exclusive backgrounds coming from rare B decays have been studied by means of large MC samples and only two channels have been found to give non-negligible contributions within the signal window: $B^0 \to \pi^0\pi^0$ and $B^0 \to \eta\pi^0$. Assuming the measured $B^0 \to \pi^0\pi^0$ branching fraction, BF($B^0 \to \pi^0\pi^0$) = $1.45 \pm 0.29 \times 10^{-6}$ [10], and the existing limit on the $B^0 \to \eta\pi^0$ branching fraction, BF($B^0 \to \eta\pi^0$) < 2.5×10^{-6} at 90% CL [10], 0.09 $B^0 \to \pi^0\pi^0$ events and less than 0.06$B^0 \to \eta\pi^0$ events at 90% CL are expected.

A two-dimensional extended unbinned maximum likelihood fit is performed on ΔE and M_{bc} to extract the signal yield. The probability density functions (PDFs) for the signal are extracted from the MC simulation. The photon energy resolution in the simulation is corrected to match the resolution measured in a photon test beam [11]. The signal PDFs are parametrized with a Crystal Ball line shape function [12] for ΔE and a double Gaussian for M_{bc}.

For the continuum background, a linear shape is assumed for ΔE, with the slope free to float in the fit, and an ARGUS [13] function for M_{bc}, with the slope parameter also free in the fit. The exclusive backgrounds enter the fit with the normalization described above. They are parametrized with a Gaussian PDF for ΔE and a double Gaussian for M_{bc}.

The fit has four free parameters: two slopes and the numbers of events of the continuum background and of the signal. It is performed within the ΔE range between -0.7 GeV and 0.6 GeV and with M_{bc} greater than 5.2 GeV/c^2. The fit window is shown in Fig. 2 as a dashed rectangle. The projections of the fit result on ΔE (with M_{bc} in its signal window) and on M_{bc} (with ΔE in its signal window) are shown in Fig. 3 as solid curves; the continuum background is shown as dashed curves, the signal as the dark shaded regions, and the exclusive backgrounds as the light shaded regions.

The signal yield is measured to be $N_{\mathrm{sig}} = 1.8^{+3.5}_{-2.7}$, corresponding to a limit on the BF of 6.1×10^{-7} at 90% CL, obtained by integration of the likelihood curve up to 90% of its total area, and including only the statistical uncertainty.

Several possible sources of systematic uncertainty are considered. Uncertainties are included in the likelihood
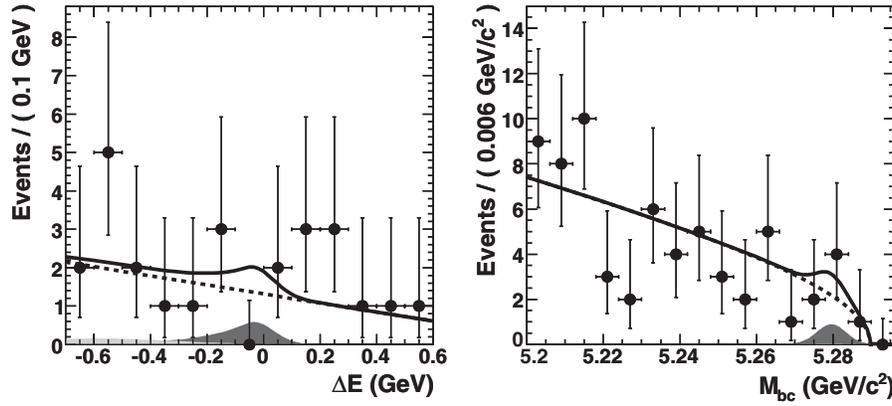
FIG. 3. Projections of the fit result on ΔE (with M_{bc} in its signal window) and on M_{bc} (with ΔE in its signal window). The fitting curve (solid line) is plotted with data (circles with error bars, drawn as asymmetric Poisson confidence intervals) and the *uds* background (dashed line). The filled regions represent the signal (dark shading) and the $B^0 \to \pi^0 \pi^0$ and $B^0 \to \eta \pi^0$ backgrounds (light shading).

TABLE I. Summary of the main systematic sources, expressed as uncertainties on the fit signal yield.

Source	Syst. unc. on N_{sig}
Signal shape	0.37
Photon rec. efficiency	0.09
LR and $\cos\theta^*$ req.	0.06
π^0 and η vetoes	0.05
Number of $B\bar{B}$ events	0.03
Background shape and norm.	0.02

function as additional parameters and then integrated over their respective ranges by assuming Gaussian probability distributions. The largest contribution is due to the modeling of the signal shape, which depends on angular and energy resolutions of the calorimeter. Uncertainties on these quantities, evaluated by studying samples of Bhabha and $e^+e^- \to \gamma\gamma$ events, have been propagated to the parameters of the signal PDFs and to the fit result. Other contributions are the uncertainties on the photon reconstruction efficiency, on event selection (LR and $\cos\theta^*$ requirements, π^0 and η mesons rejection), on the number of $B\bar{B}$ events, on background shapes, and on the normalization of the exclusive backgrounds. The separate contributions are summarized in Table I as uncertainties on the signal yield.

Inclusion of systematic uncertainties results in the following upper limit on the BF:

$$\mathrm{BF}(B^0 \to \gamma\gamma) < 6.2 \times 10^{-7} \quad \text{at } 90\% \text{ CL.}$$

In conclusion, a search for the decay $B^0 \to \gamma\gamma$ has been performed in 104 fb^{-1} of data with the Belle detector. No evidence of a signal has been observed and a new upper limit has been set, corresponding to an improvement of the previous limit of about a factor of 3.

[1] S. W. Bosch and G. Buchalla, J. High Energy Phys. 08 (2002) 054, and references therein.

[2] For a review see, in Proceedings of the 2003 SLAC Workshops (SLAC Report No. R-709), p. 60. See also:

T. M. Aliev and G. Turan, Phys. Rev. D **48**, 1176 (1993); G. G. Devidze and G. R. Jibuti, Phys. Lett. B **429**, 48 (1998); G. Devidze, A. Liparteliani, and Ulf-G. Meißner, Phys. Lett. B **634**, 59 (2006).

[3] M. Acciarri *et al.* (L3 Collaboration), Phys. Lett. B **363**, 137 (1995).

[4] B. Aubert *et al.* (*BABAR* Collaboration), Phys. Rev. Lett. **87**, 241803 (2001).

[5] S. Kurokawa and E. Kikutani, Nucl. Instrum. Methods Phys. Res., Sect. A **499**, 1 (2003), and other papers included in this volume.

[6] Y. Ushiroda (Belle SVD2 group), Nucl. Instrum. Methods Phys. Res., Sect. A **511**, 6 (2003).

[7] A. Abashian *et al.* (Belle Collaboration), Nucl. Instrum. Methods Phys. Res., Sect. A **479**, 117 (2002).

[8] S. Eidelman *et al.* (Particle Data Group), Phys. Lett. B **592**, 1 (2004).

[9] The Fox-Wolfram moments were introduced in G. C. Fox and S. Wolfram, Phys. Rev. Lett. **41**, 1581 (1978). The Fisher discriminant used by Belle, based on modified Fox-Wolfram moments, is described in K. Abe *et al.* (Belle Collaboration), Phys. Rev. Lett. **87**, 101801 (2001); Phys. Lett. B **511**, 151 (2001).

[10] E. Barberio *et al.* (Heavy Flavour Averaging Group), hep-ex/0603003.

[11] H. Ikeda *et al.*, Nucl. Instrum. Methods Phys. Res., Sect. A **441**, 401 (2000).

[12] J. E. Gaiser *et al.* (Crystal Ball Collaboration), Phys. Rev. D **34**, 711 (1986).

[13] H. Albrecht *et al.* (ARGUS Collaboration), Phys. Lett. B **241**, 278 (1990).